Analysis of three-body decays $B \to D(V \to)PP$ under the factorization-assisted topological-amplitude approach

Si-Hong Zhou[*], Run-Hui Li[†] and Xiao-Yao Lü

School of Physical Science and Technology, Inner Mongolia University, Hohhot 010021, China

Motivated by the accumulated experimental results on three-body charmed B decays with resonance contributions in *BABAR*, LHCb, and Belle (II), we systematically analyze $B_{(s)} \to D_{(s)}(V \to)P_1P_2$ decays with V representing a vector resonance (ρ, K^*, ω, or ϕ) and $P_{1,2}$ as a light pseudoscalar meson (pion or kaon). The intermediate subprocesses $B_{(s)} \to D_{(s)}V$ are calculated with the factorization-assisted topological-amplitude (FAT) approach and the intermediate resonant states V described by the relativistic Breit-Wigner distribution successively decay to P_1P_2 via strong interaction. Taking all lowest resonance states (ρ, K^*, ω, ϕ) into account, we calculate the branching fractions of these decay modes as well as the Breit-Wigner-tail effects for $B_{(s)} \to D_{(s)}(\rho, \omega \to)KK$. Our results agree with the data by *BABAR*, LHCb, and Belle (II). Among the predictions that are still not observed, there are some branching ratios of order 10^{-6}–10^{-4} which are hopeful to be measured by LHCb and Belle II. Our approach and the perturbative QCD approach (PQCD) adopt the compatible theme to deal with the resonance contributions. What is more, our data for the intermediate two-body charmed B-meson decays in FAT approach are more precise. As a result, our results for branching fractions have smaller uncertainties, especially for color-suppressed emission diagram dominated modes.

I. INTRODUCTION

Three-body nonleptonic B meson decays are not only important for the study of common topics of nonleptonic B meson decays, such as testing the standard model (SM), the studying the mechanism of CP violation and the emergence of quantum chromodynamics, but also provide opportunities for the analysis on the hadron spectroscopy. Specifically, three-body B meson decays have nontrivial kinematics and phase space distributions, which are usually described in terms of three two-body invariant mass squared combinations and two of them constitute two axes to form a Dalitz plot. In the edges of the Dalitz plot, the invariant mass squared combinations of two final-state particles will generally peak as resonances, which indicates that intermediate resonances in three-body B meson decays show up, and we are able to study the properties of these resonances through three-body B meson decays.

The Dalitz plot technique has proven to be a powerful tool to analyze the hadron spectroscopy and is widely adopted by experiments. The information on various resonance substructures including the mass, spin-parity quantum numbers, etc. have been collected by *BABAR*, Belle (II), and LHCb [1–8]. Simultaneously, usually under the framework of isobar model [9], these collaborations have also measured fit fractions of each resonance and nonresonance components. In the isobar model, the total decay amplitude can be expressed as a coherent sum of amplitudes of different resonant and nonresonant intermediate processes, where the relativistic Breit-Wigner (RBW) model usually describe resonant dynamics and exponential distribution for nonresonant terms. It is a very good approximation to adopt the RBW function for narrow width resonances which can be well separated from any other resonant or nonresonant components in the same partial wave, so that the three-body decays with narrow intermediate states, such as ρ, K^*, ω, ϕ, have been precisely measured by experiments [2–7,10–12].

On the theoretical side, analysis on the nonresonant contributions of three-body B meson decays are in an early stage of development. Approaches or models such as the heavy meson chiral perturbation theory [13–15] and a model combining the heavy quark effective theory and chiral Lagrangian [16] have been applied for calculating the nonresonant fraction of three-body charmless B meson

---

[*]Contact author: shzhou@imu.edu.cn
[†]Contact author: lirh@imu.edu.cn

decays, such as $B \to KKK$, $B \to K\pi\pi$ which are dominated by nonresonant contribution [17]. More theoretical interest is concentrated on the resonant component of three-body B decays, where two of the three final particles are produced from a resonance and recoil against the third meson called a "bachelor" meson. This type of three-body decay is also called quasi-two-body decay. Because of the large energy release in B meson decays, the two meson pair moves fast antiparallelly to the bachelor meson in the B meson rest frame. Therefore, the interactions between the meson pair and the bachelor particle are power suppressed naturally which is similar to the statement of "color transparency" in two-body B meson decays. Then approaches based on the factorization hypothesis have been proposed for calculating the quasi-two-body decays, such as the QCD factorization (QCDF) [13–15,18], the PQCD approach [19–35] and factorization-assisted topological-amplitude (FAT) approach [36,37].

In this work, we focus on three-body charmed B decays $B_{(s)} \to D_{(s)} P_1 P_2$, where $P_{1,2}$ represents a pion or kaon. Different from charmless decays, intermediate resonances in $B_{(s)} \to D_{(s)} P_1 P_2$ decays are expected to appear in the $m^2(DP_1)$ and $m^2(P_1P_2)$ combinations, thus more resonances, such as charmed states D^* and light vector or scalar resonances, can be researched simultaneously in one Dalitz plot. In addition, they provide opportunities for studies of CP violation. In particular, the Dalitz plot analysis of $B^0 \to DK^+\pi^-$ can be used as a channel to measure the unitarity triangle angle γ [38,39] and $B^0 \to \bar{D}^0\pi^+\pi^-$ is sensitive to the β angle [40,41]. Therefore, much attention has been already paid to $B_{(s)} \to D_{(s)} P_1 P_2$ decays in experiments and theoretical calculations. LHCb Collaborations have investigated structures of ground and excited states of D^*, K^* with their corresponding fit fractions through $B_{(s)} \to D_{(s)} K\pi$ [4,10], and D^*, ρ in $B_{(s)} \to D_{(s)} \pi\pi$ by BABAR and Belle [1,3]. Recently, the virtual contribution from ρ in $B_{(s)} \to D_{(s)} KK$ has been measured by Belle II [8]. Motivated by the experimental progress on $B_{(s)} \to D_{(s)} P_1 P_2$ decays, theoretical calculation on the branching fractions of various types of charmed quasi-two-body decays, $B_{(s)} \to D_{(s)} \pi\pi$, $B_{(s)} \to D_{(s)} K\pi$, and $B_{(s)} \to D_{(s)} KK$ with intermediate resonances D^*, ρ, K^*, ϕ have been completed in a series of works with the PQCD approach [42–47]. In FAT approach, we have done a systematic research on $B_{(s)} \to D_{(s)} P_1 P_2$ with ground charmed mesons D^* as the intermediate states and P_1, P_2 representing π or K [36]. The results of $B \to D^* P_2 \to D P_1 P_2$ in FAT approach are in better agreement with experimental data and more precise than the PQCD approach's predictions.

FAT approach is firstly proposed to resolve the problem about nonfactorizable contributions in two-body D and B meson decays [36,48–54] and then has been successfully generalized to quasi-two-body B meson decays [36,37].

It is based on the framework of conventional topological diagram approach, which is used to classify the decay amplitudes by different electroweak Feynman diagrams, but keeping $SU(3)$ breaking effects. Only a few unknown nonfactorization parameters need to be fitted globally with all experimental data. Therefore, FAT approach is able to provide the most precise decay amplitudes of (intermediate) two-body B meson decays especially with charmed meson final states. Then in a quasi-two-body B meson decay the intermediate resonances successively decay to final meson pairs via strong interaction, which are described in terms of the usual RBW formalism as what is done in experiments. Actually, in the PQCD approach the light cone distribution amplitude (LCDA) of a meson pair originating from a P-wave resonance can be expressed as timelike form factors and then is also parametrized by the RBW distribution. So their framework of dealing with the resonances is compatible with that in FAT. More details about this can be found in [47]. Therefore, the main difference between the FAT and the PQCD approach in quasi-two-body decays is how to calculate the intermediate two-body weak decays. It is well known that large nonperturbative contributions and power corrections expanded in m_c/m_b of color suppressed and W-exchange diagrams in charmed B decays have not been able to be calculated in PQCD approach [55], which results in large uncertainties of PQCD approach's predictions for $B \to DP_1P_2$ with resonances D^*, ρ, K^*, ϕ. In this paper we will apply FAT approach to study the $B_{(s)} \to D_{(s)} P_1 P_2$ decay with the ground state light vector intermediate resonances ρ, K^*, ϕ, ω, which are generally the largest components and their fit fractions have been well measured separately from any other vector resonances in LHCb and Belle II [1,4–8].

This paper is organized as follows. In Sec. II, the theoretical framework is introduced. The numerical results and discussions about $B_{(s)} \to D_{(s)}(\rho \to)\pi\pi$, $B_{(s)} \to D_{(s)}(K^* \to)K\pi$, $B_{(s)} \to D_{(s)}(\phi \to)K\bar{K}$, and $B_{(s)} \to D_{(s)}(\rho, \omega \to)K\bar{K}$ are collected in Sec. III. Finally, a summary is given in Sec. IV.

II. FACTORIZATION OF AMPLITUDES FOR TOPOLOGICAL DIAGRAMS

The charmed quasi-two-body decay $B_{(s)} \to D_{(s)}(V \to) P_1 P_2$ happens through two subprocesses, where the $D_{(s)}$ meson represents $D_{(s)}$ or its antiparticle $\bar{D}_{(s)}$. $B_{(s)}$ meson decays to an intermediate resonant state $D_{(s)}V$ firstly, and subsequently the unstable resonance decays to a pair of light pseudoscalar, $V \to P_1 P_2$. The first subprocess at quark level is induced by weak transitions $b \to cq\bar{u}$ ($q = d, s$) and $b \to uq\bar{c}(q = d, s)$ for $D_{(s)}$ and $\bar{D}_{(s)}$ final states, respectively. The secondary one proceeds directly by strong interaction. According to the topological structures of $b \to cq\bar{u}$, the diagrams contributing to
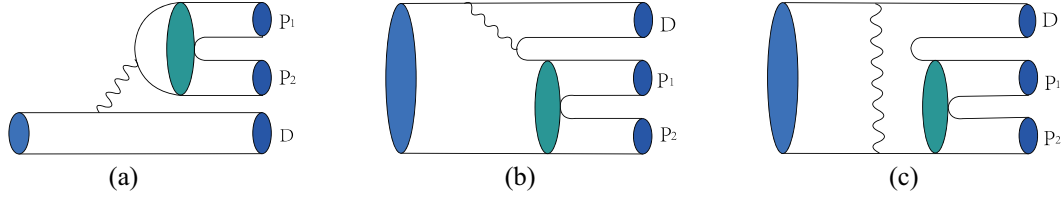
FIG. 1.   Topological diagrams of $\bar{B}_{(s)} \to D_{(s)}(V \to) P_1 P_2$ under the framework of quasi-two-body decay with the wave line representing a W boson: (a) the color-favored emission diagram T, (b) the color-suppressed emission diagram C, and (c) the W-exchange diagram E.

FIG. 2.   Topological diagrams of $\bar{B}_{(s)} \to \bar{D}_{(s)}(V \to) P_1 P_2$ under the framework of quasi-two-body decay with the wave line representing a W boson: (a) the color-favored emission diagram T, (b) the color-suppressed emission diagram C, (c) the W-exchange diagram E, and (d) W-annihilation diagram A.
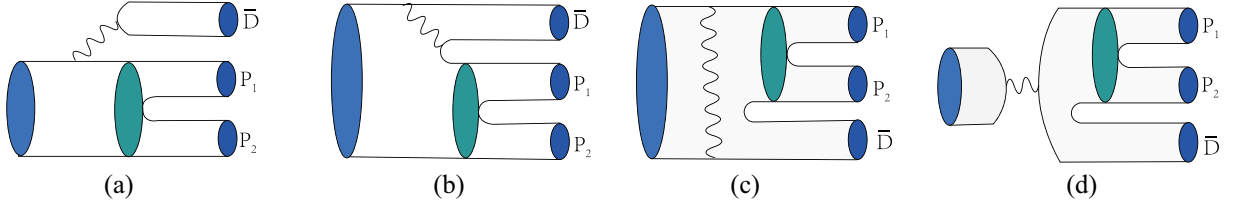
$\bar{B}_{(s)} \to D_{(s)}(V \to) P_1 P_2$ can be classified into three types as listed in Fig. 1, (a) color-favored emission diagram T, (b) color-suppressed emission diagram C, and (c) W-exchange diagram E. Similarly, besides T, C, E diagrams, the topologies of $\bar{B}_{(s)} \to \bar{D}_{(s)}(V \to) P_1 P_2$ induced by $b \to u q \bar{c}$ transitions include an additional W-annihilation diagram A as shown in Fig. 2.

The amplitudes of the first subprocess $\bar{B}_{(s)} \to D_{(s)} V$ can be referred to the ones of two-body charmed B decays in FAT approach [50]. Factorization has been proven in T topology at high precision by the QCD factorization, the perturbative QCD based on k_T factorization, together with the soft-collinear effective theory [55–57]. However, large nonfactorizable contributions have been found in C and E. As done in [50], we parametrize matrix elements of the nonfactorizable diagrams C and E in FAT approach. In case a small strong phase associated with T amplitude arise from nonfactorizable contribution such as final-state rescattering effects, it would have been included in the relative strong phase between C or E amplitude. Therefore, to reduce one free parameters, we will just apply the well proven factorization formula for T, together with parametrized C and E amplitudes, explicitly as follows,

$$T^{DV} = \sqrt{2} G_F V_{cb} V_{uq}^* a_1(\mu) f_V m_V F_1^{B \to D}(m_V^2)(\varepsilon_V^* \cdot p_B),$$

$$C^{DV} = \sqrt{2} G_F V_{cb} V_{uq}^* f_{D_{(s)}} m_V A_0^{B \to V}(m_D^2)(\varepsilon_V^* \cdot p_B) \chi^C e^{i\phi^C},$$

$$E^{DV} = \sqrt{2} G_F V_{cb} V_{uq}^* m_V f_B \frac{f_{D_{(s)}} f_V}{f_D f_\pi}(\varepsilon_V^* \cdot p_B) \chi^E e^{i\phi^E}. \quad (1)$$

So far there is not enough experimental data to do a global fit for $\bar{B}_{(s)} \to \bar{D}_{(s)} V$ decays to extract the unknown nonfactorizable parameters in the C, E amplitudes. Therefore, the same nonfactorizable parameters $\chi^C, \phi^C, \chi^E, \phi^E$ as those for $\bar{B}_{(s)} \to D_{(s)} V$ are adopted in a good approximation, just as what we do in Ref. [50]. The topological diagram A for $\bar{B}_{(s)} \to \bar{D}_{(s)} V$ is dominated by large factorizable contribution and can be calculated in the pole model [50], which is given as

$$A^{\bar{D}V} = -\sqrt{2} G_F V_{ub} V_{cq}^* a_1(\mu) f_B \frac{f_{D_{(s)}} g_{DDV} m_D^2}{m_B^2 - m_D^2}(\varepsilon_V^* \cdot p_B). \quad (2)$$

For simplification of notations, we omit the subscript (s) in $D_{(s)}$ in Eqs. (1) and (2) and the following equations except in $f_{D_{(s)}}$. $a_1(\mu)$ is the effective Wilson coefficient for the factorizable topologies T and A. $\chi^{C(E)}$ and $\phi^{C(E)}$ represent the magnitude and associated phase of $C(E)$ diagram globally fitted with the experimental data. f_V, $f_{D_{(s)}}$, and f_B are the decay constants of the corresponding vector, $D_{(s)}$ and B mesons. $F_1^{B \to D}$ and $A_0^{B \to V}$ denote the vector form factors of $B_{(s)} \to D$ and $B_{(s)} \to V$ transitions. In Eq. (2), g_{DDV} is the effective strong coupling constant and its value can be obtained from the vector meson dominance model [58], $g_{DDV} = 2.52$.

Next we will illustrate the calculation of the second subprocess, e.g., intermediate resonances decay to final states via strong interaction, $V \to P_1 P_2$. As what is done in experiments [12,59,60], we also adopt the RBW distribution for ρ, K^*, ω, and ϕ resonances, which is expressed as [15],

TABLE I. Masses m_V and full widths Γ_0 of vector resonant states [63].

Resonance	Line shape parameters	Resonance	Line shape parameters
$\rho(770)$	$m_V = 775.26 \pm 0.23$ MeV	$\omega(782)$	$m_V = 782.66 \pm 0.13$ MeV
	$\Gamma_0 = 149.1 \pm 0.8$ MeV		$\Gamma_0 = 8.68 \pm 0.13$ MeV
$K^*(892)^+$	$m_V = 891.67 \pm 0.26$ MeV	$K^*(892)^0$	$m_V = 895.55 \pm 0.20$ MeV
	$\Gamma_0 = 51.4 \pm 0.8$ MeV		$\Gamma_0 = 47.3 \pm 0.5$ MeV
$\phi(1020)$	$m_V = 1019.46 \pm 0.02$ MeV		
	$\Gamma_0 = 4.25 \pm 0.01$ MeV		

$$L^{\mathrm{RBW}}(s) = \frac{1}{s - m_V^2 + i m_V \Gamma_V(s)}, \qquad (3)$$

where s represents the invariant mass square of meson pair with 4-momenta p_1, p_2, $s = (p_1 + p_2)^2$. $\Gamma_V(s)$ represents s-dependent width of vector resonances and is defined as

$$\Gamma_V(s) = \Gamma_0 \left(\frac{q}{q_0}\right)^3 \left(\frac{m_V}{\sqrt{s}}\right) X^2(q r_{\mathrm{BW}}), \qquad (4)$$

where $X(q r_{\mathrm{BW}})$ is the Blatt-Weisskopf barrier factor,

$$X(q r_{\mathrm{BW}}) = \sqrt{[1 + (q_0 r_{\mathrm{BW}})^2]/[1 + (q r_{\mathrm{BW}})^2]}. \qquad (5)$$

In the above two equations, $q = \frac{1}{2}\sqrt{[s - (m_{P_1} + m_{P_2})^2][s - (m_{P_1} - m_{P_2})^2]/s}$ is momentum magnitude of the final state P_1 or P_2 in the rest frame of resonance V, and q_0 is just value of q when intermediate resonance is on-shell, $s = m_V^2$. While for the case that the pole mass locates outside the kinematics region, i.e., $m_V < m_{P_1} + m_{P_2}$, m_V needs to be replaced by an effective mass m_V^{eff} so that $\sqrt{s} = m_V^{\mathrm{eff}}$ for q_0. The effective mass m_V^{eff} is given by the *ad hoc* formula [61,62],

$$\begin{aligned} m_V^{\mathrm{eff}}(m_V) = m^{\min} + (m^{\max} - m^{\min}) \\ \times \left[1 + \tanh\left(\frac{m_V - \frac{m^{\min} + m^{\max}}{2}}{m^{\max} - m^{\min}}\right)\right], \end{aligned} \qquad (6)$$

where $m^{\max}$ ($m^{\min}$) is the upper (lower) boundary of the kinematics region. Another parameter together with q in $X(q r_{\mathrm{BW}})$ is the barrier radius with its value $r_{\mathrm{BW}} = 4.0~(\mathrm{GeV})^{-1}$ for all resonances [12]. Γ_0 in Eq. (4) represents the full widths of the resonant states and their values are

taken from Particle Data Group (PDG) [63] and listed in Table I together with their masses m_V.

After getting the distribution function of the vector resonances, we proceed to consider matrix element $\langle P_2(p_2)P_3(p_3)|V(p_V)\rangle$. It can be parametrized as a strong coupling constant $g_{VP_1P_2}$ which describes the strong interactions of the three mesons at hadron level. Inversely, the strong coupling constant $g_{VP_1P_2}$ can be extracted from the partial decay widths $\Gamma_{V \to P_1P_2}$ by

$$\Gamma_{V \to P_1 P_2} = \frac{2}{3} \frac{p_c^3}{4\pi m_V^2} g_{VP_1P_2}^2, \qquad (7)$$

where p_c is the magnitude of one pseudoscalar meson's momentum in the rest frame of the mother vector meson. The numerical results of $g_{\rho \to \pi^+\pi^-}$, $g_{K^* \to K^+\pi^-}$, and $g_{\phi \to K^+K^-}$ have already been directly extracted from experimental data [15],

$$g_{\rho \to \pi^+\pi^-} = 6.0, \qquad g_{K^* \to K^+\pi^-} = 4.59, \qquad g_{\phi \to K^+K^-} = -4.54. \qquad (8)$$

Those strong coupling constants, which cannot be extracted directly with experimental data, can be related to the ones in Eq. (8) by employing the quark model [64],

$$g_{\rho \to K^+K^-} : g_{\omega \to K^+K^-} : g_{\phi \to K^+K^-} = 1 : 1 : -\sqrt{2},$$

$$g_{\rho^0 \pi^+\pi^-} = g_{\rho^+\pi^0\pi^+}, \qquad g_{\rho^0\pi^0\pi^0} = g_{\omega\pi^+\pi^-} = 0,$$

$$g_{\rho^0 K^+K^-} = -g_{\rho^0 K^0\bar{K}^0} = g_{\omega K^+K^-} = g_{\omega K^0\bar{K}^0}, \qquad g_{\phi K^+K^-} = g_{\phi K^0\bar{K}^0}.$$

Finally, combining the two subprocesses together, one can get the decay amplitudes of the topological diagrams for $B \to D(V \to)P_1P_2$ shown in Figs. 1 and 2, which are given as

$$\begin{aligned} T &= \langle P_1(p_1)P_2(p_2)|(\bar{q}u)_{V-A}|0\rangle\langle D(p_D)|(\bar{c}b)_{V-A}|B(p_B)\rangle \\ &= \frac{\langle P_1(p_1)P_2(p_2)|V(p_V)\rangle}{s - m_V^2 + i m_V \Gamma_V(s)} \langle V(p_V)|(\bar{q}u)_{V-A}|0\rangle\langle D(p_D)|(\bar{c}b)_{V-A}|B(p_B)\rangle \end{aligned}$$

$$= p_D \cdot (p_1 - p_2)\sqrt{2}G_F V_{cb}V_{uq}^* a_1 f_V m_V F_1^{B\to D}(s) \frac{g_{VP_1P_2}}{s - m_V^2 + im_V\Gamma_V(s)},$$

$$C = \langle P_1(p_1)P_2(p_2)|(\bar{q}b)_{V-A}|B(p_B)\rangle\langle D(p_D)|(\bar{c}u)_{V-A}|0\rangle$$

$$= \frac{\langle P_1(p_1)P_2(p_2)|V(p_V)\rangle}{s - m_V^2 + im_V\Gamma_V(s)}\langle V(p_V)|(\bar{q}b)_{V-A}|B(p_B)\rangle\langle D(p_D)|(\bar{c}u)_{V-A}|0\rangle$$

$$= p_D \cdot (p_1 - p_2)\sqrt{2}G_F V_{cb}V_{uq}^* f_D m_V A_0^{B\to V}(m_D^2)\chi^C e^{\phi^C} \frac{g_{VP_1P_2}}{s - m_V^2 + im_V\Gamma_V(s)},$$

$$E = \langle D(p_D)P_1(p_1)P_2(p_2)|\mathcal{H}_{\text{eff}}|B(p_B)\rangle$$

$$= \frac{\langle P_1(p_1)P_2(p_2)|V(p_V)\rangle}{s - m_V^2 + im_V\Gamma_V(s)}\langle D(p_D)V(p_V)|\mathcal{H}_{\text{eff}}|B(p_B)\rangle$$

$$= p_D \cdot (p_1 - p_2)\sqrt{2}G_F V_{cb}V_{uq}^* m_V f_B \frac{f_V f_{D_{(s)}}}{f_\pi f_D}\chi^E e^{i\phi^E} \frac{g_{VP_1P_2}}{s - m_V^2 + im_V\Gamma_V(s)}, \tag{9}$$

for $b \to c$ transition, and

$$T = \langle P_1(p_1)P_2(p_2)|(\bar{u}b)_{V-A}|B(p_B)\rangle\langle \bar{D}(p_{\bar{D}})|(\bar{c}q)_{V-A}|0\rangle$$

$$= \frac{\langle P_1(p_1)P_2(p_2)|V(p_V)\rangle}{s - m_V^2 + im_V\Gamma_V(s)}\langle V(p_V)|(\bar{u}b)_{V-A}|B(p_B)\rangle\langle \bar{D}(p_{\bar{D}})|(\bar{c}u)_{V-A}|0\rangle$$

$$= p_{\bar{D}} \cdot (p_1 - p_2)\sqrt{2}G_F V_{ub}V_{cq}^* a_1 f_D m_V A_0^{B\to V}(m_D^2) \frac{g_{VP_1P_2}}{s - m_V^2 + im_V\Gamma_V(s)},$$

$$C = \langle P_1(p_1)P_2(p_2)|(\bar{u}b)_{V-A}|B(p_B)\rangle\langle \bar{D}(p_{\bar{D}})|(\bar{c}q)_{V-A}|0\rangle$$

$$= \frac{\langle P_1(p_1)P_2(p_2)|V(p_V)\rangle}{s - m_V^2 + im_V\Gamma_V(s)}\langle V(p_V)|(\bar{q}b)_{V-A}|B(p_B)\rangle\langle \bar{D}(p_{\bar{D}})|(\bar{c}u)_{V-A}|0\rangle$$

$$= p_{\bar{D}} \cdot (p_1 - p_2)\sqrt{2}G_F V_{ub}V_{cq}^* f_D m_V A_0^{B\to V}(m_D^2)\chi^C e^{i\phi^C} \frac{g_{VP_1P_2}}{s - m_V^2 + im_V\Gamma_V(s)},$$

$$E = \langle \bar{D}(p_{\bar{D}})P_1(p_1)P_2(p_2)|\mathcal{H}_{\text{eff}}|B(p_B)\rangle$$

$$= \frac{\langle P_1(p_1)P_2(p_2)|V(p_V)\rangle}{s - m_V^2 + im_V\Gamma_V(s)}\langle \bar{D}(p_{\bar{D}})V(p_V)|\mathcal{H}_{\text{eff}}|B(p_B)\rangle$$

$$= p_{\bar{D}} \cdot (p_1 - p_2)\sqrt{2}G_F V_{ub}V_{cq}^* m_V f_B \frac{f_V f_{D_{(s)}}}{f_\pi f_D}\chi^E e^{i\phi^E} \frac{g_{VP_1P_2}}{s - m_V^2 + im_V\Gamma_V(s)},$$

$$A = \langle \bar{D}(p_{\bar{D}})P_1(p_1)P_2(p_2)|\mathcal{H}_{\text{eff}}|B(p_B)\rangle$$

$$= \frac{\langle P_1(p_1)P_2(p_2)|V(p_V)\rangle}{s - m_V^2 + im_V\Gamma_V(s)}\langle \bar{D}(p_{\bar{D}})V(p_V)|\mathcal{H}_{\text{eff}}|B(p_B)\rangle$$

$$= p_{\bar{D}} \cdot (p_1 - p_2)\sqrt{2}G_F V_{ub}V_{cq}^* a_1 f_B \frac{f_D g_{DDV} m_D^2}{m_B^2 - m_D^2} \frac{g_{VP_1P_2}}{s - m_V^2 + im_V\Gamma_V(s)}, \tag{10}$$

for $b \to u$ transition, respectively. In the above equations $q = d, s$ and $p_V = p_1 + p_2 = \sqrt{s}$. The decay amplitudes of $B \to DP_1P_2$ in Eqs. (9) and (10) can also be formally written as

$$\langle D(p_D)P_1(p_1)P_2(p_2)|\mathcal{H}_{\text{eff}}|B(p_B)\rangle = p_D \cdot (p_1 - p_2)\mathcal{A}(s), \tag{11}$$

where $\mathcal{A}(s)$ represents the sub-amplitudes in Eqs. (9) and (10) with the factor $p_D \cdot (p_1 - p_2)$ taken out. The differential width of $B \to DP_1P_2$ is

$$d\Gamma = ds \frac{1}{(2\pi)^3}\frac{(|\mathbf{p_D}||\mathbf{p_1}|)^3}{6m_B^3}|\mathcal{A}(s)|^2, \tag{12}$$

where $|\mathbf{p}_D|$ and $|\mathbf{p}_1|$ represent the magnitudes of the momentum p_D and p_1, respectively. In the rest frame of the vector V resonance, their expressions are

$$|\mathbf{p_D}| = \frac{1}{2\sqrt{s}}\sqrt{(m_B^2 - m_D^2)^2 - 2(m_B^2 + m_D^2)s + s^2}$$

$$|\mathbf{p_1}| = \frac{1}{2\sqrt{s}}\sqrt{[s - (m_{P_1} + m_{P_2})^2][s - (m_{P_1} - m_{P_2})^2]}, \quad (13)$$

where $|\mathbf{p_1}| = q$.

III. NUMERICAL RESULTS AND DISCUSSION

The input parameters are classified into (a) electroweak coefficients: Cabibbo-Kobayashi-Maskawa (CKM) matrix elements and Wilson coefficients; (b) nonperturbative QCD parameters: decay constants, transition form factors and nonfactorizable parameters $\chi^{C(E)}$, $\phi^{C(E)}$; and (c) Hadronic parameters: m_V, Γ_0, and $g_{VP_1P_2}$ involved in strong inter-action decays of vector mesons, which have been listed in Table I given in previous section. The Wolfenstein para-metrization of the CKM matrix is utilized with the Wolfenstein parameters as [63]

$$\lambda = 0.22650 \pm 0.00048, \quad A = 0.790^{+0.017}_{-0.012},$$
$$\bar{\rho} = 0.141^{+0.016}_{-0.017}, \quad \bar{\eta} = 0.357 \pm 0.01.$$

The decay constants of π, K, D and B are from the PDG by global fit with experimental data [63]. The decay constants of other mesons have not been measured by experiments directly but calculated in several theoretical approaches, such as the quark model [65], the covariant light front approach [66], the light-cone sum rules [67,68], the QCD sum rules [69–75], and the lattice QCD [76–83] etc. Since the theoretical results are different in these approaches, we

choose the numerical values shown in Table II and keep a 5% uncertainty of them.

Due to absence of enough experimental data for the transition form factors of B meson decays, they have been calculated in the theoretical approaches, such as constitute quark model and light cone quark model [65,84–87], covariant light front approach(LFQM) [66,88,89], light-cone sum rules [90–111], PQCD [112–121], SCET [122], and lattice QCD [123–126] etc. Based on all above results, we list the maximum-recoil form factors in Table III, with 10% uncertainties kept in the calculation. The square of transfer momentum Q^2-dependence of form factors can be parametrized in different ways, such as the z-series parametrization applied recently for $B \to \pi, K$ in [122], $B \to \rho, \omega, K^*$ in [127] and $B_{(s)} \to D_{(s)}^{(*)}$ [128] and also pole model parametrization widely used for $B_{(s)} \to P$, $B_{(s)} \to V$ and $B_{(s)} \to D_{(s)}^{(*)}$. When dealing with (quasi-)two-body B decays, we indeed concentrate on form factor at the fixed kinematic point, so that the difference of these types of parametrization would almost have no effect. Considering the completeness of all form factors in the same para-metrization for charmed B decays, we will apply the pole model parametrization as,

$$F_i(Q^2) = \frac{F_i(0)}{1 - \alpha_1 \frac{Q^2}{m_{\text{pole}}^2} + \alpha_2 \frac{Q^4}{m_{\text{pole}}^4}}, \quad (14)$$

where F_i represents $F_{0,1}$ or A_0, and m_{pole} is the mass of the corresponding pole state, such as B^* for $F_{0,1}$ and B for A_0. $\alpha_{1,2}$ are the model parameters also shown in Table III. The effective Wilson coefficients a_1 is 1.036 calculated at scale $\mu = m_b/2$. We update the nonfactorizable parameters $\chi^{C(E)}$ and $\phi^{C(E)}$ involved in $B \to DP, D^{(*)}P, DV$ by fitting 32 updated experimental data [63]. The best-fitted values are

TABLE II. The decay constants of light pseudoscalar mesons and vector mesons (in units of MeV).

f_π	f_K	f_D	f_{D_s}	f_B	f_{B_s}	f_ρ	f_{K^*}	f_ω	f_ϕ
130.2 ± 1.7	155.6 ± 0.4	211.9 ± 1.1	258 ± 12.5	190.9 ± 4.1	225 ± 11.2	213 ± 11	220 ± 11	192 ± 10	225 ± 11

TABLE III. The transition form factors at maximum recoil and dipole model parameters.

	$F_0^{B\to\pi}$	$F_0^{B\to K}$	$F_0^{B_s\to K}$	$F_0^{B\to\eta_q}$	$F_0^{B_s\to\eta_s}$	$F_0^{B\to D}$	$F_0^{B_s\to D_s}$	$A_0^{B\to D^*}$	$A_0^{B_s\to D_s^*}$	$F_1^{B\to D}$	$F_1^{B_s\to D_s}$
$F(0)$	0.28	0.36	0.24	0.23	0.31	0.54	0.58	0.56	0.57	0.54	0.58
α_1	0.50	0.53	0.54	0.52	0.53	1.71	1.69	2.44	2.49	2.44	2.44
α_2	-0.13	-0.13	-0.15	0	0	0.52	0.78	1.98	1.74	1.49	1.70

	$F_1^{B\to\pi}$	$F_1^{B\to K}$	$F_1^{B_s\to K}$	$F_1^{B\to\eta_q}$	$F_1^{B_s\to\eta_s}$	$B_{(s)}\to V$	$A_0^{B\to\rho}$	$A_0^{B\to\omega}$	$A_0^{B_s\to\phi}$	$A_0^{B\to K^*}$	$A_0^{B_s\to K^*}$
$F(0)$	0.28	0.33	0.29	0.21	0.31	$A(0)$	0.30	0.26	0.28	0.33	0.27
α_1	0.52	0.54	0.57	1.43	1.48	α_1	1.56	1.60	1.73	1.51	1.74
α_2	0.45	0.50	0.50	0.41	0.46	α_2	0.17	0.22	0.41	0.14	0.47

$\chi^C = 0.453 \pm 0.007,$ $\phi^C = (65.06 \pm 0.83)°,$

$\chi^E = 0.023 \pm 0.001,$ $\phi^E = (142.54 \pm 5.99)°,$ (15)

with $\chi^2/\text{d.o.f.} = 1.6$.

With all the inputs, we integrate the differential width in Eq. (12) over the kinematics region to obtain the branching fractions of $\bar{B} \to D(V \to)P_1P_2$ and $\bar{B} \to \bar{D}(V \to)P_1P_2$. Specifically, the numerical results for $\bar{B}_{(s)} \to D(\rho \to)\pi\pi$, $\bar{B}_{(s)} \to D(K^* \to)K\pi$, $\bar{B}_{(s)} \to D(\phi \to)KK$, and $\bar{B}_{(s)} \to D(\rho, \omega \to)KK$, together with their corresponding doubly CKM suppressed decays $\bar{B} \to \bar{D}(V \to)P_1P_2$, are collected in Tables IV–VII, respectively. In our results denoted by $\mathcal{B}_{\text{FAT}}$, the uncertainties are in sequence from the fitted parameters, form factors, decay constants for $\bar{B} \to D(V \to)P_1P_2$, and an additional error from V_{ub} in the last one for $\bar{B} \to \bar{D}(V \to)P_1P_2$ decays induced by $b \to u$ transitions. The errors from hadronic parameters, the masses and decay widths of vector mesons, can be ignored. One can see that the dominating errors are from the uncertainties of form factors, which can be improved by more precise calculations. Besides the CKM matrix elements shown in these tables, we also list the intermediate resonance decays as well as the topological contributions T, C, E, and A for convenience of analyzing hierarchies of branching fractions in the following. Experimental data in

the third column and the results in PQCD approach in last column are also list for comparison.

A. Hierarchies of branching fractions

The decay modes are classified by CKM matrix elements involved, Cabibbo favored $V_{cb}V_{ud}^*$, Cabibbo suppressed $V_{cb}V_{us}^*$, and doubly Cabibbo suppressed $V_{ub}V_{ud}^*$ and $V_{ub}V_{us}^*$, shown in the second column of Tables IV–VI. The hierarchies of branching fractions can be seen clearly from this classification. The Cabibbo favored decay modes are about two orders larger than the doubly Cabibbo suppressed ones of the same type in the same table. As a result, these Cabibbo favored decay modes are able to be measured first by experiments, such as the first four modes of $\bar{B}_{(s)} \to D(\rho \to)\pi\pi$ [63] in Table IV and $\bar{B}_s^0 \to D^0(K^{*0} \to)K^+\pi^-$ [4] in Table V. Our results and the experimental data are consistent within errors.

Besides CKM matrix elements, the hierarchy of branching fraction is also dependent on contributions from different topological diagrams. Similar to the dynamics of two-body hadronic B decays, the color favored emission diagram (T) is absolutely dominating in the quasi-two-body decays. For instance, the topology T dominated decay modes, $B^- \to D^0(K^{*-} \to)K^-\pi^0$, $\bar{B}^0 \to D^+(K^{*-} \to)K^-\pi^0$ and $\bar{B}_s^0 \to D_s^+(K^{*-} \to)K^-\pi^0$ happening through Cabibbo suppressed $V_{cb}V_{us}^*$, are the same order as the Cabibbo favored but only C contributed decay,

TABLE IV. Branching ratios in FAT approach of quasi-two-body decays (top) $\bar{B}_{(s)} \to D(\rho \to)\pi\pi$ ($\times10^{-4}$) with the uncertainties from the fitted parameters, form factors and decay constants, respectively, and (bottom) $\bar{B}_{(s)} \to \bar{D}(\rho \to)\pi\pi$ ($\times10^{-6}$) with one more error from V_{ub} in the last one, together with results in PQCD and experimental data for comparision. The CKM matrix elements and characters T, C, E, and A representing the corresponding topological diagram contributions are also listed in the second column.

Decay modes	Amplitudes	Data	$\mathcal{B}_{\text{FAT}}$	$\mathcal{B}_{\text{PQCD}}$
$\bar{B} \to D(\rho \to)\pi\pi$	$V_{cb}V_{ud}^*$			
$B^- \to D^0(\rho^- \to)\pi^0\pi^-$	$T+C$	134 ± 18	$90.8^{+1.5+16.1+8.1}_{-1.5-15.0-7.8}$	115^{+59}_{-38}
$\bar{B}^0 \to D^+(\rho^- \to)\pi^0\pi^-$	$T+E$	76 ± 12	$58.4^{+0.5+12.9+6.2}_{-0.5-11.6-5.9}$	$82.3^{+49.2}_{-29.0}$
$\bar{B}^0 \to D^0(\rho^0 \to)\pi^+\pi^-$	$\frac{1}{\sqrt{2}}(E-C)$	3.21 ± 0.21	$2.40^{+0.13+0.22+0.03}_{-0.13-0.45-0.03}$	$1.39^{+1.24}_{-0.90}$
$\bar{B}_s^0 \to D_s^+(\rho^- \to)\pi^-\pi^0$	T	95 ± 20	$74.5^{+0.0+15.6+7.9}_{-0.0-14.2-7.5}$	$77.2^{+40.2}_{-25.6}$
	$V_{cb}V_{us}^*$			
$\bar{B}_s^0 \to D^+(\rho^- \to)\pi^-\pi^0$	E		$0.016^{+0.003+0+0.005}_{-0.001-0-0.004}$	$0.051^{+0.022}_{-0.014}$
$\bar{B}_s^0 \to D^0(\rho^0 \to)\pi^+\pi^-$	$\frac{1}{\sqrt{2}}E$		$0.008^{+0.001+0+0.002}_{-0.001-0-0.001}$	$0.026^{+0.010}_{-0.006}$
$\bar{B} \to \bar{D}(\rho \to)\pi\pi$	$V_{ub}V_{cs}^*$			
$B^- \to D_s^-(\rho^0 \to)\pi^+\pi^-$	$\frac{1}{\sqrt{2}}T$		$16.7^{+0.0+3.5+1.7+1.5}_{-0.0-3.2-1.6-1.5}$	$15.2^{+11.1}_{-8.2}$
$\bar{B}^0 \to D_s^-(\rho^+ \to)\pi^+\pi^0$	T		$29.7^{+0.0+6.2+2.9+2.6}_{-0.0-5.6-2.8-2.6}$	$28.2^{+20.4}_{-15.3}$
$\bar{B}_s^0 \to D^-(\rho^+ \to)\pi^+\pi^0$	E		$0.17^{+0.02+0+0.02+0.02}_{-0.01-0-0.02-0.02}$	$0.69^{+0.20}_{-0.16}$
$\bar{B}_s^0 \to \bar{D}^0(\rho^0 \to)\pi^+\pi^-$	$\frac{1}{\sqrt{2}}E$		$0.09^{+0.01+0+0.01+0.01}_{-0.01-0-0.01-0.01}$	$0.34^{+0.10}_{-0.08}$
	$V_{ub}V_{cd}^*$			
$B^- \to D^-(\rho^0 \to)\pi^+\pi^-$	$\frac{1}{\sqrt{2}}(T-A)$		$0.35^{+0+0.10+0.01+0.03}_{-0-0.09-0.01-0.03}$	$0.53^{+0.36}_{-0.27}$
$B^- \to \bar{D}^0(\rho^- \to)\pi^+\pi^0$	$C+A$		$0.41^{+0.01+0.06+0.01+0.04}_{-0.01-0.06-0.01-0.04}$	$0.05^{+0.02}_{-0.01}$
$\bar{B}^0 \to D^-(\rho^+ \to)\pi^+\pi^0$	$T+E$		$0.99^{+0.01+0.22+0.01+0.09}_{-0.01-0.20-0.01-0.09}$	$0.76^{+0.59}_{-0.31}$
$\bar{B}^0 \to \bar{D}^0(\rho^0 \to)\pi^+\pi^-$	$\frac{1}{\sqrt{2}}(E-C)$		$0.10^{+0.01+0.02+0+0.001}_{-0.01-0.02-0-0.001}$	$0.013^{+0.009}_{-0.008}$

TABLE V. The same as table IV, but for the quasi-two-body decays (top) $\bar{B}_{(s)} \to D(K^* \to)K\pi$ ($\times 10^{-4}$), and (bottom) $\bar{B}_{(s)} \to \bar{D}(K^* \to)K\pi$ ($\times 10^{-6}$).

Decay modes	Amplitudes	Data	$\mathcal{B}_{\text{FAT}}$	$\mathcal{B}_{\text{PQCD}}$
$\bar{B} \to D(K^* \to)K\pi$	$V_{cb}V_{ud}^*$			
$\bar{B}^0 \to D_s^+(K^{*-} \to)K^-\pi^0$	E		$0.10^{+0.01+0+0.02}_{-0.01-0-0.01}$	$0.52^{+0.14+0.05+0.05}_{-0.12-0.08-0.00}$
$\bar{B}_s^0 \to D^0(K^{*0} \to)K^+\pi^-$	C	2.86 ± 0.44	$3.33^{+0.10+0.70+0.03}_{-0.10-0.63-0.03}$	$2.86^{+1.67+0.43+0.05}_{-1.33-0.56-0.08}$
	$V_{cb}V_{us}^*$			
$B^- \to D^0(K^{*-} \to)K^-\pi^0$	$T+C$		$1.89^{+0.03+0.33+0.16}_{-0.03-0.31-0.16}$	$1.67^{+0.71+0.32+0.07}_{-0.53-0.34-0.07}$
$\bar{B}^0 \to D^+(K^{*-} \to)K^-\pi^0$	T		$1.31^{+0+0.28+0.13}_{-0-0.25-0.13}$	$1.24^{+0.55+0.15+0.06}_{-0.40-0.18-0.05}$
$\bar{B}^0 \to D^0(\bar{K}^{*0} \to)K^-\pi^+$	C	0.32 ± 0.05	$0.24^{+0.01+0.05+0.003}_{-0.01-0.05-0.003}$	$0.17^{+0.10+0.03+0.00}_{-0.08-0.03-0.01}$
$\bar{B}_s^0 \to D_s^+(K^{*-} \to)K^-\pi^0$	$T+E$		$1.38^{+0.01+0.31+0.14}_{-0.01-0.28-0.14}$	$1.11^{+0.45+0.20+0.05}_{-0.33-0.21-0.04}$
$\bar{B} \to \bar{D}(K^* \to)K\pi$	$V_{ub}V_{cs}^*$			
$B^- \to \bar{D}^0(K^{*-} \to)K^-\pi^0$	$C+A$		$3.83^{+0.12+0.64+0.05+0.34}_{-0.12-0.59-0.05-0.39}$	$1.00^{+0.43+0.20+0.00}_{-0.48-0.27-0.07}$
$B^- \to D^-(\bar{K}^{*0} \to)K^-\pi^+$	A		$0.72^{+0+0+0.03+0.06}_{-0-0-0.01-0.06}$	$0.21^{+0.10+0.03+0.04}_{-0.06-0.02-0.00}$
$\bar{B}^0 \to \bar{D}^0(\bar{K}^{*0} \to)K^-\pi^+$	C		$3.10^{+0.10+0.65+0.03+0.27}_{-0.10-0.59-0.03-0.27}$	$1.96^{+1.01+0.52+0.11}_{-0.87-0.41-0.12}$
$\bar{B}_s^0 \to D_s^-(K^{*+} \to)K^+\pi^0$	$T+E$		$8.11^{+0.15+1.87+0.82+0.72}_{-0.16-1.68-0.77-0.72}$	$13.3^{+6.84+0.76+0.80}_{-3.04-0.73-0.79}$
	$V_{ub}V_{cd}^*$			
$B^- \to D_s^-(K^{*0} \to)K^+\pi^-$	A		$0.037^{+0+0+0.002+0.003}_{-0-0-0.001-0.003}$	$0.014^{+0.008+0.004+0.002}_{-0.003-0.008-0.0002}$
$\bar{B}^0 \to D_s^-(K^{*+} \to)K^+\pi^0$	E		$0.005^{+0.0004+0+0.0007+0.0004}_{-0.0004-0-0.0006+0.0004}$	$0.005^{+0.003+0.001+0}_{-0.003-0.001-0}$
$\bar{B}_s^0 \to D^-(K^{*+} \to)K^+\pi^0$	T		$0.35^{+0+0.07+0.004+0.03}_{-0-0.07-0.004+0.03}$	$0.6^{+0.30+0.03+0.04}_{-0.15-0.04-0.04}$
$\bar{B}_s^0 \to \bar{D}^0(K^{*0} \to)K^+\pi^-$	C		$0.15^{+0.01+0.03+0.002+0.01}_{-0.01-0.03-0.002-0.01}$	$0.08^{+0.05+0.02+0.00}_{-0.03-0.02-0.00}$

TABLE VI. The same as Table IV, but for the quasi-two-body decays (top) $\bar{B}_{(s)} \to D(\phi \to)KK$ ($\times 10^{-4}$), and (bottom) $\bar{B}_{(s)} \to \bar{D}(\phi \to)KK$ ($\times 10^{-6}$).

Decay modes	Amplitudes	$\mathcal{B}_{\text{FAT}}$	$\mathcal{B}_{\text{PQCD}}$
$\bar{B} \to D(\phi \to)KK$	$V_{cb}V_{us}^*$		
$\bar{B}_s^0 \to D^0(\phi \to)K^+K^-$	C	$0.150^{+0.005+0.031+0.002}_{-0.005-0.028-0.002}$	
$\to D^0(\phi \to)K^0\bar{K}^0$		$0.104^{+0.003+0.022+0.001}_{-0.003-0.020-0.001}$	
$\bar{B} \to D(\phi \to)KK$	$V_{ub}V_{cs}^*$		
$B^- \to D_s^-(\phi \to)K^+K^-$	A	$0.75^{+0+0+0.32+0.07}_{-0-0-0.32-0.07}$	$0.15^{+0.02+0.01+0.01}_{-0.02-0.01-0.01}$
$\to D_s^-(\phi \to) \to K^0K^0$		$0.52^{+0+0+0.32+0.05}_{-0-0-0.34-0.05}$	$0.10^{+0.01+0.01+0.01}_{-0.01-0.01-0.01}$
$\bar{B}_s^0 \to \bar{D}^0(\phi \to)K^+K^-$	C	$2.21^{+0.07+0.82+0.02+0.19}_{-0.07-0.42-0.02-0.19}$	
$\to \bar{D}^0(\phi \to)\bar{K}^0K^0$		$1.54^{+0.05+0.57+0.02+0.14}_{-0.05-0.29-0.02-0.14}$	

$\bar{B}_s^0 \to D^0(K^{*0} \to)K^+\pi^-$. Besides the mode $\bar{B}_s^0 \to D^0(K^{*0} \to)K^+\pi^-$ with large branching ration has been measured by LHCb experiment through Dalitz plot analysis and isobar model [4], another mode $\bar{B}^0 \to D^0(\bar{K}^{*0} \to)K^-\pi^+$ with one order smaller branching ration is also measured by LHCb [6]. The remaining three modes with comparable branching ratio as $\bar{B}_s^0 \to D^0(K^{*0} \to)K^+\pi^-$ are also measurable in LHCb and Belle II. Our results of other decays, especially those with branching ratios in the range 10^{-6}–10^{-4} in Tables IV–VI are expected to be observed in future experiments.

B. Comparison with the results in the PQCD approach

Since most quasi-two-body decays $B_{(s)} \to D_{(s)}(V \to)P_1P_2$ have not been measured by experiments until now,

we list the results calculated in PQCD approach [42,43,45–47] in the last column of the tables for comparison. As we have stated in Sec. I, LCDA of P-wave P_1P_2 meson pair from resonance is described by RBW model in PQCD, which is the same theme adopted in the FAT approach for $V \to P_1P_2$. The two approaches are effectively compatible for intermediate resonance strong decays, the main difference between them is the calculation of the weak decays of B to D meson and a vector resonance.

As known, T diagram is proved to be factorizable at all orders of α_s for these decays, thus the perturbative calculation is reliable. Our results of the T diagram dominating decay modes in Tables IV and V are in good agreement with PQCD's predictions. The magnitude of topologies C is larger than E, $|C| > |E|$, in the FAT

TABLE VII. Comparison of results from FAT ($\mathcal{B}_{\mathrm{FAT}}^v$) and PQCD ($\mathcal{B}_{\mathrm{PQCD}}^v$) approach for the virtual effects of $B_{(s)} \to D(\rho, \omega \to)K\bar{K}$ decays, happened when the pole masses of ρ, ω are smaller than the invariant mass of $K\bar{K}$.

Decay modes	$\mathcal{B}_{\mathrm{FAT}}^v$	$\mathcal{B}_{\mathrm{PQCD}}^v$
$\bar{B} \to D(\rho \to)KK$		
$B^- \to D^0(\rho^- \to)K^-K^0$	$6.59^{+0.10+1.21+0.61}_{-0.09-1.12-0.60} \times 10^{-5}$	$11.8^{+6.2+0.9+0.7}_{-4.0-1.2-0.9} \times 10^{-5}$
$\bar{B}^0 \to D^+(\rho^- \to)K^-K^0$	$4.54^{+0.03+0.99+0.48}_{-0.03-0.89-0.46} \times 10^{-5}$	$7.93^{+5.01+0.32+0.65}_{-2.93-0.30-0.63} \times 10^{-5}$
$\bar{B}^0 \to D^0(\rho^0 \to)K^+K^-$	$1.28^{+0.07+0.12+0.01}_{-0.07-0.24-0.01} \times 10^{-6}$	$1.07^{+0.46+0.80+0.01}_{-0.37-0.58-0.01} \times 10^{-6}$
$\bar{B}_s^0 \to D_s^+(\rho^- \to)K^-K^0$	$5.63^{+0+1.18+0.60}_{-0-1.07-0.60} \times 10^{-5}$	$6.06^{+3.47+0.04+0.47}_{-2.06-0.04-0.45} \times 10^{-5}$
$\bar{B}_s^0 \to D^+(\rho^- \to)K^-K^0$	$8.68^{+0.77+0+2.52}_{-0.74-0-1.76} \times 10^{-9}$	$4.22^{+0.58+0.90+0.40}_{-0.67-0.65-0.30} \times 10^{-8}$
$\bar{B}_s^0 \to D^0(\rho^0 \to)K^+K^-$	$0.44^{+0.04+0+0.10}_{-0.04-0-0.06} \times 10^{-8}$	$1.05^{+0.15+0.23+0.10}_{-0.17-0.15-0.07} \times 10^{-8}$
$\bar{B} \to \bar{D}(\rho \to)KK$		
$B^- \to D^-(\rho^0 \to)K^+K^-$	$1.89^{+0+0.53+0.03+0.04}_{-0-0.46-0.03-0.04} \times 10^{-9}$	$3.22^{+0.52+0.86+0.01}_{-0.45-0.43-0.01} \times 10^{-9}$
$B^- \to \bar{D}^0(\rho^- \to)K^-K^0$	$2.15^{+0.07+0.31+0.04+0.19}_{-0.07-0.29-0.03-0.19} \times 10^{-9}$	$0.53^{+0.12+0.25+0.03}_{-0.06-0.17-0.01} \times 10^{-9}$
$B^- \to D_s^-(\rho^0 \to)K^+K^-$	$8.74^{+0+1.83+0.87+0.77}_{-0-1.66-0.83-0.77} \times 10^{-8}$	$6.26^{+1.69+2.69+0.03}_{-1.30-0.92-0.02} \times 10^{-8}$
$\bar{B}^0 \to D^-(\rho^+ \to)K^+K^0$	$5.15^{+0.07+1.16+0.06+0.05}_{-0.08-1.04-0.06-0.05} \times 10^{-9}$	$6.87^{+2.05+3.30+0.08}_{1.60-1.01-0.08} \times 10^{-9}$
$\bar{B}^0 \to \bar{D}^0(\rho^0 \to)K^+K^-$	$5.49^{+0.31+1.16+0.06+0.48}_{-0.30-1.04-0.06-0.48} \times 10^{-10}$	$0.78^{+0.20+0.46+0.08}_{-0.13-0.29-0.06} \times 10^{-10}$
$\bar{B}^0 \to D_s^-(\rho^+ \to)K^+K^0$	$1.51^{+0+0.32+0.15+0.13}_{-0-0.29-0.14-0.13} \times 10^{-7}$	$2.32^{+0.63+1.00+0.01}_{-0.48-0.34-0.01} \times 10^{-7}$
$\bar{B}_s^0 \to D^-(\rho^+ \to)K^+K^0$	$0.99^{+0.17+0+0.11+0.09}_{-0.08-0-0.11-0.09} \times 10^{-9}$	$7.47^{+1.49+2.42+0.40}_{-0.32-1.83-0.37} \times 10^{-9}$
$\bar{B}_s^0 \to \bar{D}^0(\rho^0 \to)K^+K^-$	$0.51^{+0.09+0+0.06+0.04}_{-0.04-0-0.05-0.04} \times 10^{-9}$	$1.85^{+0.36+0.61+0.09}_{-0.32-0.45-0.08} \times 10^{-9}$
$\bar{B} \to D(\omega \to)KK$		
$\bar{B}^0 \to D^0(\omega \to)K^+K^-$	$1.54^{+0.08+0.13+0.02}_{-0.07-0.27-0.02} \times 10^{-6}$	
$\bar{B}_s^0 \to D^0(\omega \to)K^+K^-$	$3.68^{+0.33+0+0.84}_{-0.31-0-0.53} \times 10^{-9}$	
$\bar{B} \to \bar{D}(\omega \to)KK$		
$B^- \to D_s^-(\omega \to)K^+K^-$	$6.90^{+0+1.45+0.68+0.61}_{-0-1.31-0.65-0.61} \times 10^{-8}$	
$B^- \to D^-(\omega \to)K^+K^-$	$4.15^{+0+0.68+0.06+0.37}_{-0-0.63-0.05-0.37} \times 10^{-9}$	
$\bar{B}^0 \to \bar{D}^0(\omega \to)K^+K^-$	$5.16^{+0.26+1.00+0.07+0.46}_{-0.25-0.91-0.07-0.46} \times 10^{-10}$	
$\bar{B}_s^0 \to \bar{D}^0(\omega \to)K^+K^-$	$3.87^{+0.34+0+0.46+0.34}_{-0.33-0-0.41-0.37} \times 10^{-10}$	

approach as shown in Eq. (15), while C is approximately equal to E, $|C| \sim |E|$, in the PQCD approach [129], because it is sensitive to the power corrections and high order contributions which are hard to be calculated in PQCD approach. Therefore, it is easy to find in Tables IV and V that the results of the FAT approach for the decays dominated only by C, larger than those in the PQCD approach, are in better agreement with the current experimental data. However, our results of decay modes with only power suppressed E contribution are a little smaller than those in PQCD, which need to be tested by the future experiments. At last, we emphasize that the branching ratios of decays in the FAT approach are more precise than those in the PQCD in Tables IV–VI. The reason is that the topological amplitudes in the FAT including the nonfactorizable QCD contributions were extracted through a global fit with experimental data of these decays, while large uncertainties arise from nonperturbative parameters and QCD power and radiative corrections in the PQCD.

C. The virtual effects of $B_{(s)} \to D(\rho, \omega \to)K\bar{K}$

Contrary to the quasi-two-body decays through $\rho \to \pi\pi$, $K^* \to K\pi$ and $\phi \to KK$ proceeding by the pole mass

dynamics, i.e., the pole mass is larger than the invariant mass threshold of two final states, the other modes with strong decays by $\rho, \omega \to KK$ can only happen by ρ, ω off-shell effect. It is also called the Breit-Wigner tail (BWT) effect, which has also appeared in charmed quasi-two-body decay with off-shell D^* resonance [36,44] and charmless one through ρ, ω resonances [21–23,25,37]. We denote branching ratios of this kind of decays by $\mathcal{B}^v$ and their numerical results are listed on Table VII, together with the PQCD's predictions for $B \to D(\rho \to)KK$ in last column.

Apparently, the branching ratios of $\mathcal{B}^v$ modes are approximately two orders smaller than those of $\mathcal{B}$ modes in Table IV, that is, the BWT effect in $B \to D(\rho \to)KK$ is only about 1% of the on-shell resonance contribution, $B \to D(\rho \to)\pi\pi$. In Tables VI and VII, one can see that all the intermediate states of ρ, ω, and ϕ can decay into KK via virtual effects (for ρ, ω) or pole mass dynamics (for ϕ). However, different from neutral states ρ^0, ω, ϕ, the charged $\rho^\pm$ is the unique resonance contributing to the charged meson pair $K^\pm K^0$ in the low mass region of $K^\pm K^0$ system, which have been measured recently by Belle II collaboration [8] based on a study of the small $m(K^- K_S^0)$ invariant mass

for $B^- \to D^0 K^- K^0_S$ and $\bar{B}^0 \to D^+ K^- K^0_S$. With ρ^--like resonances and nonresonance contribution, the branching ratios are $\mathcal{B}(B^- \to D^0 K^- K^0_S) = (1.89 \pm 0.16 \pm 0.10) \times 10^{-4}$ and $\mathcal{B}(\bar{B}^0 \to D^+ K^- K^0_S) = (0.85 \pm 0.11 \pm 0.05) \times 10^{-4}$, respectively. Our result for only ground state $\rho(770)$ is $\mathcal{B}(B^- \to D^0 (\rho^- \to) K^- K^0) = (7.01^{+0.13+1.26+0.63}_{-0.14-1.16-0.60}) \times 10^{-5}$ and $\mathcal{B}(B^- \to D^0 (\rho^- \to) K^- K^0) = (4.64^{+0.03+1.00+0.49}_{-0.02-0.90-0.47}) \times 10^{-5}$ in Table VII, which can reach a proportion of about 20% of above measured all ρ^- resonant and nonresonant components (considering half of branching ratios of K^0 or $\bar{K}^0$ to become K_S). The similar mode $\bar{B}^0_s \to D^+_s (\rho^- \to) K^- K^0$ with comparable branching ratio $(5.63^{+0+1.18+0.60}_{-0-1.07-0.60}) \times 10^{-5}$ is suggested to be measured in LHCb and Belle II.

The study of invariant mass of neutral $K^+ K^-$ system for $\bar{B} \to D K^+ K^-$ in experiments is relatively complex, as it involves various resonances ρ^0, ω and ϕ as well as nonresonances. Especially, in the low-mass region of $m(K^+ K^-)$, the BWT effects from neutral resonance ρ^0 and ω in decay modes such as $\bar{B}^0 \to D^0 (\rho^0 \to) K^+ K^-$ and $\bar{B}^0 \to D^0 (\omega \to) K^+ K^-$, $\bar{B}^0_s \to D^0 (\rho^0 \to) K^+ K^-$ and $\bar{B}^0_s \to D^0 (\omega \to) K^+ K^-$, are pretty much the same in Table VII, even though the decay widths of ρ and ω meson are very different, shown in Table I. As we have mentioned in [36,37], the BWT effects in these decays are not very sensitive to the widths of resonances. It can be attributed to the behavior of the Breit-Wigner propagator in Eq. (3) describing off-shell resonance, where the invariant mass square s is far away from the on-shell mass of resonance, e.g. the real part, $|s - m_{\rho,\omega}|$, of denominators of Breit-Wigner formula is much larger than the imaginary part $im_{\rho,\omega}\Gamma_{\rho,\omega}$.

Finally, the comparison of BWT effect in $B \to D(\rho \to) KK$ between the FAT and PQCD approaches is very similar with that of the on-shell resonance contributions in $B \to D(\rho \to) \pi\pi$. They are in agreement for T diagram dominated modes, but different from those dominated by C and E diagrams. It indicates again that no matter for on-shell resonance or for off-shell one, the mechanisms or models applied by the two approaches are effectively consistent.

IV. CONCLUSION

Motivated by the measurements of three-body charmed B meson decays with resonance contributions, especially ground state resonance contributions, from *BABAR*, LHCb, and Belle (II), we systematically analyze the corresponding quasi-two-body decays $B_{(s)} \to D_{(s)} (V \to) P_1 P_2$

through intermediate ground states ρ, K^*, ω and ϕ. They proceed by $b \to c$ or $b \to u$ transitions to a $D_{(s)} V$ intermediate state with V as a resonant state which decays consequently into final states P_1, P_2 via strong interaction. We utilize the decay amplitudes extracted from the two-body charmed B decays in the FAT approach for the first subprocess $B_{(s)} \to D_{(s)} V$ and RBW function for the narrow widths resonances V as usually done in experiments and the PQCD approach. We categorize $B_{(s)} \to D_{(s)} (V \to) P_1 P_2$ into four groups according to different vector resonance, $B_{(s)} \to D_{(s)} (\rho \to) \pi\pi$, $B_{(s)} \to D_{(s)} (K^* \to) K\pi$, $B_{(s)} \to D_{(s)} (\phi \to) KK$ and $B_{(s)} \to D_{(s)} (\rho, \omega \to) KK$, where the former three kinds of modes decay by pole dynamics, and the last one by BWT effect.

We calculate the branching ratios of all the four kinds of decay modes in the FAT method. Our results are consistent with the data by *BABAR*, LHCb, and Belle (II). Our predictions of order 10^{-6}–10^{-4} without any experimental data are hopeful to be observed in the future experiments. The FAT approach and the PQCD approach have effectively compatible mechanism of resonant state strong decays. Meanwhile, their treatments on the weak decays of B to a D meson and a vector resonance are different. Since the calculation of the first subprocess is done by a global fit with experimental data in the FAT approach, our results for the color suppressed diagram dominating modes are larger than those in the PQCD approach whose information on nonperturbative contribution and m_c/m_b power corrections are not included so far. In addition, our results have significantly less theoretical uncertainties due to accurate nonfactorizable parameters extracted from experimental data.

The fourth type of modes happen through the tail effects of ρ and ω resonance to KK. It is found that the BWT effect of ρ resonance approximately is about two orders smaller than ρ on-shell resonance contribution, which induce that they are usually ignored in experimental analysis. However charged $\rho^\pm$-like resonance of low mass region of $K^\pm K^0$ system have been started to be studied in Belle II recently. The comparable modes, such as $\bar{B}^0_s \to D^+_s (\rho^- \to) K^- K^0$, also have the potential to be measurable in LHCb and Belle II.

[1] A. Kuzmin *et al.* (Belle Collaboration), Study of anti-$B^0 \rightarrow D^0\pi^+\pi^-$ decays, Phys. Rev. D **76**, 012006 (2007).

[2] B. Aubert *et al.* (BABAR Collaboration), Dalitz plot analysis of $B^- \rightarrow D^+\pi^-\pi^-$, Phys. Rev. D **79**, 112004 (2009).

[3] P. del Amo Sanchez *et al.* (BABAR Collaboration), Dalitz-plot analysis of $B^0 \rightarrow \bar{D}^0\pi^+\pi^-$, arXiv:1007.4464.

[4] R. Aaij *et al.* (LHCb Collaboration), Dalitz plot analysis of $B_s^0 \rightarrow \bar{D}^0K^-\pi^+$ decays, Phys. Rev. D **90**, 072003 (2014).

[5] R. Aaij *et al.* (LHCb Collaboration), Dalitz plot analysis of $B^0 \rightarrow \bar{D}^0\pi^+\pi^-$ decays, Phys. Rev. D **92**, 032002 (2015).

[6] R. Aaij *et al.* (LHCb Collaboration), Amplitude analysis of $B^0 \rightarrow \bar{D}^0K^+\pi^-$ decays, Phys. Rev. D **92**, 012012 (2015).

[7] R. Aaij *et al.* (LHCb Collaboration), Observation of the decay $B_s^0 \rightarrow \bar{D}^0K^+K^-$, Phys. Rev. D **98**, 072006 (2018).

[8] F. Abudinén *et al.* (Belle-II Collaboration), Observation of $B \rightarrow D^{(*)}K^-K_S^0$ decays using the 2019–2022 Belle II data sample, arXiv:2305.01321.

[9] D. J. Herndon, P. Söding, and R. J. Cashmore, Generalized isobar model formalism, Phys. Rev. D **11**, 3165 (1975).

[10] R. Aaij *et al.* (LHCb Collaboration), First observation of the decay $\bar{B}_s^0 \rightarrow D^0K^{*0}$ and a measurement of the ratio of branching fractions $\frac{\mathcal{B}(\bar{B}_s^0 \rightarrow D^0K^{*0})}{\mathcal{B}(\bar{B}^0 \rightarrow D^0\rho^0)}$, Phys. Lett. B **706**, 32 (2011).

[11] J. P. Lees *et al.* (BABAR Collaboration), Evidence for *CP* violation in $B^+ \rightarrow K^*(892)^+\pi^0$ from a Dalitz plot analysis of $B^+ \rightarrow K_S^0\pi^+\pi^0$ decays, Phys. Rev. D **96**, 072001 (2017).

[12] R. Aaij *et al.* (LHCb Collaboration), Amplitude analysis of the $B^+ \rightarrow \pi^+\pi^+\pi^-$ decay, Phys. Rev. D **101**, 012006 (2020).

[13] H.-Y. Cheng and K.-C. Yang, Nonresonant three-body decays of D and B mesons, Phys. Rev. D **66**, 054015 (2002).

[14] H.-Y. Cheng, C.-K. Chua, and A. Soni, Charmless three-body decays of B mesons, Phys. Rev. D **76**, 094006 (2007).

[15] H.-Y. Cheng and C.-K. Chua, Branching fractions and direct *CP* violation in charmless three-body decays of B mesons, Phys. Rev. D **88**, 114014 (2013).

[16] S. Fajfer, T.-N. Pham, and A. Prapotnik, *CP* violation in the partial width asymmetries for $B^- \rightarrow \pi^+\pi^-K^-$ and $B^- \rightarrow K^+K^-K^-$ decays, Phys. Rev. D **70**, 034033 (2004).

[17] H.-Y. Cheng, Theoretical overview of hadronic three-body B decays, arXiv:0806.2895.

[18] T. Huber, J. Virto, and K. K. Vos, Three-body non-leptonic heavy-to-heavy *B* decays at NNLO in QCD, J. High Energy Phys. 11 (2020) 103.

[19] C.-H. Chen and H.-n. Li, Three body nonleptonic B decays in perturbative QCD, Phys. Lett. B **561**, 258 (2003).

[20] W.-F. Wang, H.-C. Hu, H.-n. Li, and C.-D. Lü, Direct *CP* asymmetries of three-body *B* decays in perturbative QCD, Phys. Rev. D **89**, 074031 (2014).

[21] W.-F. Wang and H.-n. Li, Quasi-two-body decays $B \rightarrow K\rho \rightarrow K\pi\pi$ in perturbative QCD approach, Phys. Lett. B **763**, 29 (2016).

[22] Y. Li, A.-J. Ma, W.-F. Wang, and Z.-J. Xiao, Quasi-two-body decays $B_{(s)} \rightarrow P\rho \rightarrow P\pi\pi$ in perturbative QCD approach, Phys. Rev. D **95**, 056008 (2017).

[23] Y. Li, W.-F. Wang, A.-J. Ma, and Z.-J. Xiao, Quasi-two-body decays $B_{(s)} \rightarrow K^*(892)h \rightarrow K\pi h$ in perturbative QCD approach, Eur. Phys. J. C **79**, 37 (2019).

[24] W.-F. Wang, Will the subprocesses $\rho(770, 1450)^0 \rightarrow K^+K^-$ contribute large branching fractions for $B^\pm \rightarrow \pi^\pm K^+K^-$ decays?, Phys. Rev. D **101**, 111901(R) (2020).

[25] Y.-Y. Fan and W.-F. Wang, Resonance contributions $\phi(1020, 1680) \rightarrow K\bar{K}$ for the three-body decays $B \rightarrow K\bar{K}h$, Eur. Phys. J. C **80**, 815 (2020).

[26] W.-F. Wang, Contributions for the kaon pair from $\rho(770)$, $\omega(782)$ and their excited states in the $B \rightarrow K\bar{K}h$ decays, Phys. Rev. D **103**, 056021 (2021).

[27] Z.-T. Zou, Y. Li, Q.-X. Li, and X. Liu, Resonant contributions to three-body $B \rightarrow KKK$ decays in perturbative QCD approach, Eur. Phys. J. C **80**, 394 (2020).

[28] Z.-T. Zou, Y. Li, and X. Liu, Branching fractions and *CP* asymmetries of the quasi-two-body decays in $B_s \rightarrow K^0(\bar{K}^0)K^\pm\pi^\mp$ within PQCD approach, Eur. Phys. J. C **80**, 517 (2020).

[29] Z.-T. Zou, L. Yang, Y. Li, and X. Liu, Study of quasi-two-body $B_{(s)} \rightarrow \phi(f_0(980)/f_2(1270) \rightarrow)\pi\pi$ decays in perturbative QCD approach, Eur. Phys. J. C **81**, 91 (2021).

[30] L. Yang, Z.-T. Zou, Y. Li, X. Liu, and C.-H. Li, Quasi-two-body $B_{(s)} \rightarrow V\pi\pi$ decays with resonance $f_0(980)$ in the PQCD approach, Phys. Rev. D **103**, 113005 (2021).

[31] W.-F. Liu, Z.-T. Zou, and Y. Li, Charmless quasi-two-body B decays in perturbative QCD approach: Taking $B \rightarrow KR \rightarrow K^+K^-$ as examples, Adv. High Energy Phys. **2022**, 5287693 (2022).

[32] Z.-Q. Zhang, Y.-C. Zhao, Z.-L. Guan, Z.-J. Sun, Z.-Y. Zhang, and K.-Y. He, Quasi-two-body decays in the perturbative QCD approach*, Chin. Phys. C **46**, 123105 (2022).

[33] Z.-Y. Zhang, Z.-Q. Zhang, S.-Y. Wang, Z.-J. Sun, and Y.-Y. Yang, Quasi-two-body decays Bc → K∗h → Kπh in perturbative QCD, Phys. Rev. D **108**, 076009 (2023).

[34] Y.-C. Zhao, Z.-Q. Zhang, Z.-Y. Zhang, Z.-J. Sun, and Q.-B. Meng, Quasi-two-body decays in perturbative QCD*, Chin. Phys. C **47**, 073104 (2023).

[35] Q. Chang, L. Yang, Z.-T. Zou, and Y. Li, Study of the $B^+ \rightarrow \pi^+(\pi^+\pi^-)$ decay in PQCD approach, Eur. Phys. J. C **84**, 753 (2024).

[36] S.-H. Zhou, R.-H. Li, Z.-Y. Wei, and C.-D. Lu, Analysis of three-body charmed B-meson decays under the factorization-assisted topological-amplitude approach, Phys. Rev. D **104**, 116012 (2021).

[37] S.-H. Zhou, X.-X. Hai, R.-H. Li, and C.-D. Lu, Analysis of three-body charmless B-meson decays under the factorization-assisted topological-amplitude approach, Phys. Rev. D **107**, 116023 (2023).

[38] T. Gershon, On the measurement of the unitarity triangle angle γ from $B^0 \rightarrow DK^{*0}$ decays, Phys. Rev. D **79**, 051301 (2009).

[39] T. Gershon and M. Williams, Prospects for the measurement of the unitarity triangle angle gamma from $B_0 \rightarrow DK^+\pi^-$ decays, Phys. Rev. D **80**, 092002 (2009).

[40] B. Aubert *et al.* (BABAR Collaboration), Measurement of $\cos 2\beta$ in $B^0 \rightarrow D^{(*)}h^0$ decays with a time-dependent Dalitz plot analysis of $D \rightarrow K_S^0\pi^+\pi^-$, Phys. Rev. Lett. **99**, 231802 (2007).

[41] P. Krokovny *et al.* (Belle Collaboration), Measurement of the quark mixing parameter $\cos 2\phi_1$ using time-dependent Dalitz analysis of anti-$B^0 \to D[K^0_{(s)}\pi^+\pi^-]h^0$, Phys. Rev. Lett. **97**, 081801 (2006).

[42] A.-J. Ma, Y. Li, W.-F. Wang, and Z.-J. Xiao, The quasi-two-body decays $B_{(s)} \to (D_{(s)}.\bar{D}_{(s)})\rho \to (D_{(s)}.\bar{D}_{(s)})\pi\pi$ in the perturbative QCD factorization approach, Nucl. Phys. **B923**, 54 (2017).

[43] A.-J. Ma, Resonances $\phi(1020)$ and $\phi(1680)$ contributions for the three-body decays $B^+ \to D^+_s K\bar{K}$, Int. J. Mod. Phys. A **35**, 2050164 (2020).

[44] J. Chai, S. Cheng, and W.-F. Wang, The role of $D^*_{(s)}$ and their contributions in $B_{(s)} \to D_{(s)}hh'$ decays, Phys. Rev. D **103**, 096016 (2021).

[45] Z.-T. Zou, W.-S. Fang, X. Liu, and Y. Li, Analysis of CKM-favored quasi-two-body $B \to D(R \to)K\pi$ decays in PQCD approach, Eur. Phys. J. C **82**, 1076 (2022).

[46] W.-S. Fang, Z.-T. Zou, and Y. Li, Phenomenological analysis of the quasi-two-body B → D(R →)Kπ decays in PQCD approach, Phys. Rev. D **108**, 113007 (2023).

[47] W.-F. Wang, L.-F. Yang, A.-J. Ma, and A. Ramos, The low-mass enhancement of kaon pairs in $B^+ \to \bar{D}^{(*)0}K^+\bar{K}^0$ and $B^0 \to D^{(*)-}K^+\bar{K}^0$ decays, Phys. Rev. D **109**, 116009 (2024).

[48] H.-n. Li, C.-D. Lu, and F.-S. Yu, Branching ratios and direct *CP* asymmetries in $D \to PP$ decays, Phys. Rev. D **86**, 036012 (2012).

[49] Q. Qin, H.-n. Li, C.-D. Lü, and F.-S. Yu, Branching ratios and direct *CP* asymmetries in $D \to PV$ decays, Phys. Rev. D **89**, 054006 (2014).

[50] S.-H. Zhou, Y.-B. Wei, Q. Qin, Y. Li, F.-S. Yu, and C.-D. Lu, Analysis of two-body charmed *B* meson decays in factorization-assisted topological-amplitude approach, Phys. Rev. D **92**, 094016 (2015).

[51] S.-H. Zhou, Q.-A. Zhang, W.-R. Lyu, and C.-D. Lü, Analysis of charmless two-body B decays in factorization assisted topological amplitude approach, Eur. Phys. J. C **77**, 125 (2017).

[52] H.-Y. Jiang, F.-S. Yu, Q. Qin, H.-n. Li, and C.-D. Lü, $D^0 - \bar{D}^0$ mixing parameter y in the factorization-assisted topological-amplitude approach, Chin. Phys. C **42**, 063101 (2018).

[53] S.-H. Zhou and C.-D. Lü, Extraction of the CKM phase γ from the charmless two-body *B* meson decays, Chin. Phys. C **44**, 063101 (2020).

[54] Q. Qin, C. Wang, D. Wang, and S.-H. Zhou, The factorization-assisted topological-amplitude approach and its applications, Front. Phys. (Beijing) **18**, 64602 (2023).

[55] Y.-Y. Keum, T. Kurimoto, H. N. Li, C.-D. Lu, and A. I. Sanda, Nonfactorizable contributions to $\bar{B}D^{(*)}M$ M decays, Phys. Rev. D **69**, 094018 (2004).

[56] M. Beneke, G. Buchalla, M. Neubert, and C. T. Sachrajda, QCD factorization for exclusive, nonleptonic B meson decays: General arguments and the case of heavy light final states, Nucl. Phys. **B591**, 313 (2000).

[57] C. W. Bauer, D. Pirjol, and I. W. Stewart, A proof of factorization for B → Dπ, Phys. Rev. Lett. **87**, 201806 (2001).

[58] Z. Lin and C. M. Ko, Model for j/ψ absorption in hadronic matter, Phys. Rev. C **62**, 034903 (2000).

[59] J. P. Lees *et al.* (*BABAR* Collaboration), Amplitude analysis of $B^0 \to K^+\pi^-\pi^0$ and evidence of direct *CP* violation in $B \to K^*\pi$ decays, Phys. Rev. D **83**, 112010 (2011).

[60] J. P. Lees *et al.* (*BABAR* Collaboration), Precise measurement of the $e^+e^- \to \pi^+\pi^-(\gamma)$ cross section with the initial-state radiation method at *BABAR*, Phys. Rev. D **86**, 032013 (2012).

[61] R. Aaij *et al.* (LHCb Collaboration), Dalitz plot analysis of $B^0_s \to \bar{D}^0 K^-\pi^+$ decays, Phys. Rev. D **90**, 072003 (2014).

[62] R. Aaij *et al.* (LHCb Collaboration), Amplitude analysis of $B^- \to D^+\pi^-\pi^-$ decays, Phys. Rev. D **94**, 072001 (2016).

[63] R. L. Workman *et al.* (Particle Data Group), Review of particle physics, Prog. Theor. Exp. Phys. **2022**, 083C01 (2022) and 2024 update.

[64] C. Bruch, A. Khodjamirian, and J. H. Kuhn, Modeling the pion and kaon form factors in the timelike region, Eur. Phys. J. C **39**, 41 (2005).

[65] R. C. Verma, Decay constants and form factors of s-wave and p-wave mesons in the covariant light-front quark model, J. Phys. G **39**, 025005 (2012).

[66] H.-Y. Cheng, C.-K. Chua, and C.-W. Hwang, Covariant light front approach for s wave and p wave mesons: Its application to decay constants and form-factors, Phys. Rev. D **69**, 074025 (2004).

[67] P. Ball, G. W. Jones, and R. Zwicky, $B \to V\gamma$ beyond QCD factorisation, Phys. Rev. D **75**, 054004 (2007).

[68] A. Bharucha, D. M. Straub, and R. Zwicky, $B \to V\ell^+\ell^-$ in the standard model from light-cone sum rules, J. High Energy Phys. 08 (2016) 098.

[69] M. Jamin and B. O. Lange, f_B and $f_{B_{(s)}}$ from QCD sum rules, Phys. Rev. D **65**, 056005 (2002).

[70] P. Gelhausen, A. Khodjamirian, A. A. Pivovarov, and D. Rosenthal, Decay constants of heavy-light vector mesons from QCD sum rules, Phys. Rev. D **88**, 014015 (2013); **89**, 099901(E) (2014); **91**, 099901(E) (2015).

[71] W. Lucha, D. Melikhov, and S. Simula, Decay constants of the charmed vector mesons D^* and D^*_s from QCD sum rules, Phys. Lett. B **735**, 12 (2014).

[72] A. A. Penin and M. Steinhauser, Heavy light meson decay constant from QCD sum rules in three loop approximation, Phys. Rev. D **65**, 054006 (2002).

[73] S. Narison, c, b quark masses and $f_{D_{(s)}}$, $f_{B_{(s)}}$ decay constants from pseudoscalar sum rules in full QCD to order α_s^2, Phys. Lett. B **520**, 115 (2001).

[74] W. Lucha, D. Melikhov, and S. Simula, Decay constants of heavy pseudoscalar mesons from QCD sum rules, J. Phys. G **38**, 105002 (2011).

[75] S. Narison, A fresh look into $m_{c,b}$ and precise $f_{D(s),B(s)}$ from heavy-light QCD spectral sum rules, Phys. Lett. B **718**, 1321 (2013).

[76] R. J. Dowdall, C. T. H. Davies, R. R. Horgan, C. J. Monahan, and J. Shigemitsu (HPQCD Collaboration), B-meson decay constants from improved lattice nonrelativistic QCD with physical u, d, s, and c quarks, Phys. Rev. Lett. **110**, 222003 (2013).

[77] N. Carrasco *et al.*, A $N_f = 2 + 1 + 1$ "twisted" determination of the *b*-quark mass, f_B and f_{B_s}, Proc. Sci. LATTICE2013 (**2014**) 313 [arXiv:1311.2837].

[78] P. Dimopoulos *et al.* (ETM Collaboration), Lattice QCD determination of m_b, f_B and f_{B_s} with twisted mass Wilson fermions, J. High Energy Phys. 01 (2012) 046.

[79] C. McNeile, C. T. H. Davies, E. Follana, K. Hornbostel, and G. P. Lepage, High-precision f_{B_s} and HQET from relativistic lattice QCD, Phys. Rev. D **85**, 031503 (2012).

[80] A. Bazavov *et al.* (Fermilab Lattice and MILC Collaborations), B- and D-meson decay constants from three-flavor lattice QCD, Phys. Rev. D **85**, 114506 (2012).

[81] H. Na, C. J. Monahan, C. T. H. Davies, R. Horgan, G. P. Lepage, and J. Shigemitsu, The B and B_s meson decay constants from lattice QCD, Phys. Rev. D **86**, 034506 (2012).

[82] A. Bussone *et al.*, Lattice QCD study of B-meson decay constants from ETMC, in *8th International Workshop on the CKM Unitarity Triangle* (2014), arXiv:1411.5566.

[83] F. Bernardoni *et al.* (ALPHA Collaboration), Decay constants of B-mesons from non-perturbative HQET with two light dynamical quarks, Phys. Lett. B **735**, 349 (2014).

[84] D. Melikhov and B. Stech, Weak form-factors for heavy meson decays: An update, Phys. Rev. D **62**, 014006 (2000).

[85] C. Q. Geng, C.-W. Hwang, C. C. Lih, and W. M. Zhang, Mesonic tensor form-factors with light front quark model, Phys. Rev. D **64**, 114024 (2001).

[86] C.-D. Lu, W. Wang, and Z.-T. Wei, Heavy-to-light form factors on the light cone, Phys. Rev. D **76**, 014013 (2007).

[87] C. Albertus, Weak decays of $\bar{B}_s$ mesons, Phys. Rev. D **89**, 065042 (2014).

[88] H.-Y. Cheng and C.-K. Chua, B to V, A, T tensor form factors in the covariant light-front approach: Implications on radiative B decays, Phys. Rev. D **81**, 114006 (2010); **82**, 059904(E) (2010).

[89] C.-H. Chen, Y.-L. Shen, and W. Wang, $|V_{ub}|$ and $B \to \eta^{\prime}$ form factors in covariant light front approach, Phys. Lett. B **686**, 118 (2010).

[90] P. Ball and V. M. Braun, Exclusive semileptonic and rare B meson decays in QCD, Phys. Rev. D **58**, 094016 (1998).

[91] P. Ball, $B \to \pi$ and $B \to K$ transitions from QCD sum rules on the light cone, J. High Energy Phys. 09 (1998) 005.

[92] P. Ball and R. Zwicky, Improved analysis of $B \to \pi e \nu$ from QCD sum rules on the light cone, J. High Energy Phys. 10 (2001) 019.

[93] P. Ball and R. Zwicky, New results on $B \to \pi, K, \eta$ decay formfactors from light-cone sum rules, Phys. Rev. D **71**, 014015 (2005).

[94] P. Ball and R. Zwicky, $B_{d,s} \to \rho, \omega, K^*, \phi$ decay form-factors from light-cone sum rules revisited, Phys. Rev. D **71**, 014029 (2005).

[95] P. Ball and G. W. Jones, $B \to \eta^{(\prime)}$ form factors in QCD, J. High Energy Phys. 08 (2007) 025.

[96] J. Charles, A. Le Yaouanc, L. Oliver, O. Pene, and J. C. Raynal, Heavy to light form-factors in the heavy mass to large energy limit of QCD, Phys. Rev. D **60**, 014001 (1999).

[97] A. Bharucha, T. Feldmann, and M. Wick, Theoretical and phenomenological constraints on form factors for radiative and semi-leptonic B-meson decays, J. High Energy Phys. 09 (2010) 090.

[98] A. Bharucha, Two-loop corrections to the $B \to \pi$ form factor from QCD sum rules on the light-cone and $|V_{ub}|$, J. High Energy Phys. 05 (2012) 092.

[99] A. Khodjamirian, T. Mannel, and N. Offen, Form-factors from light-cone sum rules with B-meson distribution amplitudes, Phys. Rev. D **75**, 054013 (2007).

[100] A. Khodjamirian, T. Mannel, N. Offen, and Y. M. Wang, $B \to \pi \ell \nu_l$ width and $|V_{ub}|$ from QCD light-cone sum rules, Phys. Rev. D **83**, 094031 (2011).

[101] Y.-M. Wang and Y.-L. Shen, QCD corrections to $B \to \pi$ form factors from light-cone sum rules, Nucl. Phys. **B898**, 563 (2015).

[102] U.-G. Meißner and W. Wang, Generalized heavy-to-light form factors in light-cone sum rules, Phys. Lett. B **730**, 336 (2014).

[103] Y.-L. Wu, M. Zhong, and Y.-B. Zuo, $B_{(s)}, D_{(s)} \to \pi, K, \eta, \rho, K^*, \omega, \phi$ transition form factors and decay rates with extraction of the CKM parameters $|V_{ub}|, |V_{cs}|, |V_{cd}|$, Int. J. Mod. Phys. A **21**, 6125 (2006).

[104] X.-G. Wu and T. Huang, Radiative corrections on the $B \to P$ form factors with chiral current in the light-cone sum rules, Phys. Rev. D **79**, 034013 (2009).

[105] G. Duplancic, A. Khodjamirian, T. Mannel, B. Melic, and N. Offen, Light-cone sum rules for $B \to \pi$ form factors revisited, J. High Energy Phys. 04 (2008) 014.

[106] M. A. Ivanov, J. G. Korner, S. G. Kovalenko, P. Santorelli, and G. G. Saidullaeva, Form factors for semileptonic, nonleptonic and rare $B(B_s)$ meson decays, Phys. Rev. D **85**, 034004 (2012).

[107] M. Ahmady, R. Campbell, S. Lord, and R. Sandapen, Predicting the $B \to K^*$ form factors in light-cone QCD, Phys. Rev. D **89**, 074021 (2014).

[108] H.-B. Fu, X.-G. Wu, and Y. Ma, $B \to K^*$ transition form factors and the semi-leptonic decay $B \to K^* \mu^+ \mu^-$, J. Phys. G **43**, 015002 (2016).

[109] Y.-M. Wang, Y.-B. Wei, Y.-L. Shen, and C.-D. Lü, Perturbative corrections to B $\to$ D form factors in QCD, J. High Energy Phys. 06 (2017) 062.

[110] C.-D. Lü, Y.-L. Shen, Y.-M. Wang, and Y.-B. Wei, QCD calculations of $B \to \pi, K$ form factors with higher-twist corrections, J. High Energy Phys. 01 (2019) 024.

[111] J. Gao, T. Huber, Y. Ji, C. Wang, Y.-M. Wang, and Y.-B. Wei, B $\to$ D$\ell \nu_\ell$ form factors beyond leading power and extraction of $|V_{cb}|$ and R_D, J. High Energy Phys. 05 (2022) 024.

[112] H.-n. Li, Y.-L. Shen, and Y.-M. Wang, Next-to-leading-order corrections to $B \to \pi$ form factors in k_T factorization, Phys. Rev. D **85**, 074004 (2012).

[113] W.-F. Wang and Z.-J. Xiao, The semileptonic decays $B/B_s \to (\pi, K)(\ell^+ \ell^-, \ell \nu, \nu \bar{\nu})$ in the perturbative QCD approach beyond the leading-order, Phys. Rev. D **86**, 114025 (2012).

[114] W.-F. Wang, Y.-Y. Fan, M. Liu, and Z.-J. Xiao, Semi-leptonic decays $B/B_s \to (\eta, \eta^\prime, G)(l^+ l^-, l\bar{\nu}, \nu\bar{\nu})$ in the perturbative QCD approach beyond the leading order, Phys. Rev. D **87**, 097501 (2013).

[115] Y.-Y. Fan, W.-F. Wang, S. Cheng, and Z.-J. Xiao, Semi-leptonic decays $B \to D^{(*)} l \nu$ in the perturbative QCD factorization approach, Chin. Sci. Bull. **59**, 125 (2014).

[116] Y.-Y. Fan, W.-F. Wang, and Z.-J. Xiao, Study of $\bar{B}_s^0 \to (D_s^+, D_s^{*+})l^-\bar{\nu}_l$ decays in the pQCD factorization approach, Phys. Rev. D **89,** 014030 (2014).

[117] T. Kurimoto, H.-n. Li, and A. I. Sanda, Leading power contributions to $B \to \pi, \rho$ transition form-factors, Phys. Rev. D **65,** 014007 (2002).

[118] T. Kurimoto, H.-n. Li, and A. I. Sanda, $B \to D^{(*)}$ form-factors in perturbative QCD, Phys. Rev. D **67,** 054028 (2003).

[119] C.-D. Lu and M.-Z. Yang, B to light meson transition form-factors calculated in perturbative QCD approach, Eur. Phys. J. C **28,** 515 (2003).

[120] Z.-T. Wei and M.-Z. Yang, The systematic study of $B \to \pi$ form-factors in pQCD approach and its reliability, Nucl. Phys. **B642,** 263 (2002).

[121] T. Huang and X.-G. Wu, Consistent calculation of the $B \to \pi$ transition form-factor in the whole physical region, Phys. Rev. D **71,** 034018 (2005).

[122] B.-Y. Cui, Y.-K. Huang, Y.-L. Shen, C. Wang, and Y.-M. Wang, Precision calculations of $B_{d,s} \to \pi$, K decay form factors in soft-collinear effective theory, J. High Energy Phys. 03 (2023) 140.

[123] R. R. Horgan, Z. Liu, S. Meinel, and M. Wingate, Lattice QCD calculation of form factors describing the rare decays $B \to K^*\ell^+\ell^-$ and $B_s \to \phi\ell^+\ell^-$, Phys. Rev. D **89,** 094501 (2014).

[124] E. Dalgic, A. Gray, M. Wingate, C. T. H. Davies, G. P. Lepage, and J. Shigemitsu, B meson semileptonic form-factors from unquenched lattice QCD, Phys. Rev. D **73,** 074502 (2006); **75,** 119906(E) (2007).

[125] L. Lellouch, Flavor physics and lattice quantum chromo-dynamics, in *Les Houches Summer School: Session 93: Modern Perspectives in lattice QCD: Quantum Field Theory and High Performance Computing* (2011), pp. 629–698, arXiv:1104.5484.

[126] S. Aoki *et al.*, Review of lattice results concerning low-energy particle physics, Eur. Phys. J. C **74,** 2890 (2014).

[127] J. Gao, C.-D. Lü, Y.-L. Shen, Y.-M. Wang, and Y.-B. Wei, Precision calculations of $B \to V$ form factors from soft-collinear effective theory sum rules on the light-cone, Phys. Rev. D **101,** 074035 (2020).

[128] B.-Y. Cui, Y.-K. Huang, Y.-M. Wang, and X.-C. Zhao, Shedding new light on R(D(s)(∗)) and $\left|V_{cb}\right|$ from semi-leptonic B⁻(s) → D(s)(∗)ℓν⁻ℓ decays, Phys. Rev. D **108,** L071504 (2023).

[129] R.-H. Li, C.-D. Lu, and H. Zou, The $B(B_s) \to D_{(s)}P, D_{(s)}V, D_{(s)}^*P,$ and $D_{(s)}^*V$ decays in the perturbative QCD approach, Phys. Rev. D **78,** 014018 (2008).